ISBN: 978-3-95450-168-7 doi:10.18429/JACoW-IPAC2015-MOPJE036

LONGITUDINAL IMPEDANCE CHARACTERIZATION OF THE CERN SPS VACUUM FLANGES

José E. Varela, CERN, Geneva, Switzerland

Abstract

This contribution describes the thorough studies carried out to characterize the longitudinal impedance of the CERN SPS vacuum flanges, which are believed to be the main source of LHC beam instability. Around 600 high-impedance flanges of 12 different types have been identified. Not only, full-wave electromagnetic field simulations, but also RF measurements have been used to evaluate the impedance of these elements. The R/Q of the relevant resonances was measured using the well-known bead-pull technique. In particular, a subset of $\sim$ 150 flanges has been found to be the source of a high-impedance resonance at 1.4 GHz, also observed in beam measurements. Two possible ways of reducing the impedance of these elements are currently under consideration and will be briefly discussed here.

INTRODUCTION

Longitudinal multi-bunch instability in the CERN SPS with a very low intensity threshold is a serious limitation for the future doubling of bunch intensity required by the HL-LHC project. During the past years, a lot of effort has been put into studying this instability by means of beam dynamics simulations [1]. Self-evidently, these simulations rely on having an accurate impedance model of the machine. This contribution describes the longitudinal coupling impedance of the elements which are believed to be the source of the instability.

The longitudinal coupling impedance of the interconnects between the different types of vacuum chambers in the SPS was already studied by G. Dôme in 1973 [2]. As a result, cylindrical resistors were placed all around the ring to damp the resonances created by the aforementioned interconnects. In 2001, around 800 pumping ports were shielded in a huge impedance reduction campaign as they were limiting the performance of the SPS [3]. Currently, the multi-bunch instability threshold is reached at $\sim 3 \times 10^{10}$ p/b. To reach the nominal intensity of 1.15×10^{11} both, the 800 MHz cavities and controlled longitudinal emittance blow up are used. The SPS bunches will be too long for the LHC to capture for the requested intensity of HL-LHC (2.5×10^{11}). As part of the LHC Injectors Upgrade (LIU) project [4], one of the potential cures for this problem is to reduce the impedance of the vacuum flanges [5].

LONGITUDINAL COUPLING IMPEDANCE CHARACTERIZATION

Classification of the Vacuum Flanges

The vacuum flanges in the SPS can be divided in two main groups depending on the vacuum chambers that they interconnect. Small (83 mm inner diameter) circular cross-section chambers are referred to as QD beam pipes. Similarly, elliptical and quasi-rectangular cross sections are named QF and MBA beam pipes. Flanges interconnecting two QD vacuum chambers, as the one shown in Fig. 1 (a), belong to group I. On the other hand, flanges interconnecting any combination of MBA and QF chambers, see Fig. 1 (b) and (c), belong to group II. Groups I and II contain approximately 400 and 240 flanges respectively. Each group is further divided into six different flange types. Finally, a number of flanges in the SPS have an enamel coating. The enamel is used to electrically isolate both sides of the flange. These flanges are part of the grounding scheme of the SPS which minimizes the effect of eddy currents.

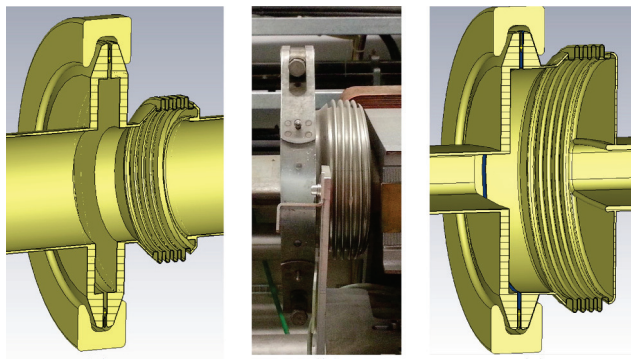

Figure 1: SPS vacuum flanges. (a) Model of a QD-QD flange. (b) Photo of a QF-MBA flange in the SPS. (c) Model of an MBA-MBA flange.

Simulations

All the aforementioned types have been modeled using official SPS layouts and simulated using HFSS [6], CST [7] or both. As analogous to the method used to calculate beam-loading in the CLIC main Linac [8], an on-axis plane wave was used as a source to calculate the beam induced field inside the enameled interconnects. Non-enameled flanges were characterized using both the aforementioned method and the wake field solver of CST. The enamel coating was modeled as a 0.2 mm thick layer with relative permeability $\epsilon_r = 3$ and dielectric losses $\tan\delta = 0.01$. Finally, a conductivity of $\sigma = 1.35 \times 10^6$ S/m was used for the beam pipes and bellows to model the 304L/316L stainless steel.

Flanges belonging to group II are responsible for a set of resonances around 1.4 GHz. The enameled flanges are open and inhomogeneous resonators. Radiation losses were found to be dominant in all enameled flanges of group II. On top of this, these flanges have damping resistors inside. The damping resistors are hollow alumina cylinders with

ISBN: 978-3-95450-168-7 doi:10.18429/JACoW-IPAC2015-MOPJE036

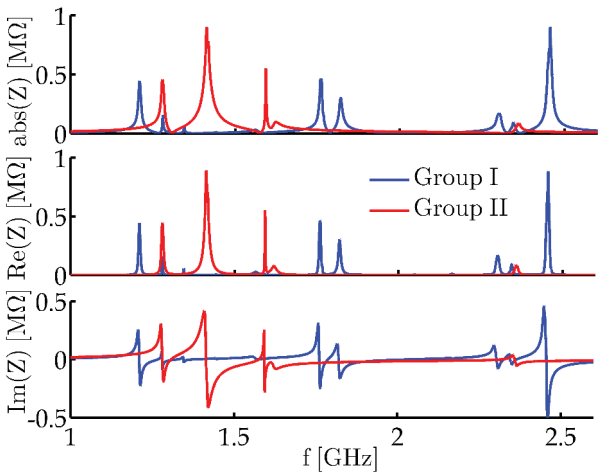

Figure 2: Total Longitudinal Coupling Impedance of the vacuum flanges in the SPS. The blue and red lines show the contribution of flanges belonging to groups I and II respectively.

a nickel-chrome coating which could not be accounted for in simulations reliably. During the last Christmas technical stop, an x-ray survey was launched to check the presence of these elements in the machine. Around 12% of the surveyed positions didn't have resistors. Even though, the enamel coating and the damping resistors greatly damp these resonances they still maintain their high R/Q (from 75 to 80 Ω). Thus, flanges belonging to group II are responsible for the single-bunch instability observed in the SPS.

Group I is responsible for a set of high-Q resonances around 2.3 GHz. Even though there is a high number of enameled flanges in this group, the 2.3 GHz resonance is located in the additional volume created by the particular way in which the bellows are welded to the vacuum chamber, see Fig. 1 (a). Therefore, this resonance doesn't 'see' the enamel coating and, consequently, is not damped. The R/Q of these resonances ranges from 10 to 20 Ω (4 to 8 times smaller than before). Since these are the only known high-Q elements in the ring they are, most likely, driving the multi-bunch instabilities observed in the SPS.

Figure 2 shows the total longitudinal impedance of 365 and 200 interconnects belonging to groups I and II, respectively. As aforementioned, the main contributions from groups I and II are the peaks at 2.3 and 1.4 GHz respectively. However, group I also has non-negligible impedance peaks around 1.2 and 1.8 GHz and group II also resonates around 1.3 and 1.6 GHz. The impedance plot shown in Fig. 2 takes into account the resonant frequency scatter produced by the different extrusion/compression of the bellows where appropriate. Typically, a 2.5 to 5% scatter has been applied, depending on the length of the bellows. Only the 1.6 GHz resonance of group II is unaffected by this, since this peak comes from 21 non-enameled interconnects that do not have bellows.

Table 1: Simulations and measurements of a non-enameled (closed) MBA-QF and an enameled MBA-MBA flange.

		Damping resistor	f_0 [GHz]	Q_0	R/Q [Ω]
Closed	Sim.	No	1.415	1800	82
	Meas.	No	1.401	1470	85 ± 2%
	Meas.	Yes	1.395	200	81 ± 5%
Enameled	Sim.	No	1.410	285	75
	Meas.	No	1.415	270	79 ± 5%
	Meas.	Yes	1.415	75	65 ± 5%

Measurements

Bead-pull measurements [9], were carried out to asses the simulation results of two representative flange types belonging to group II, namely the enameled MBA-MBA and non-enameled (closed) MBA-QF flanges. These two types were chosen because of their high R/Q, to evaluate the accuracy of the simulation results for enameled flanges and to measure the Q of the resonances with and without damping resistor. Table 1 summarizes the obtained results. Note that the uncertainty of the measurements is higher for low-Q resonances.

Three main conclusions can be drawn from the measurement results. First, there is a very good agreement between the simulated and measured R/Q values for both flanges (without damping resistors). Second, the simulation results for the enameled case are very accurate. All three f_0, Q_0 and R/Q values are nicely predicted. Finally, the damping resistors heavily damp the high-Q resonance of the non-enameled case, but seem to 'saturate' and damp proportionally less for the enameled interconnect. In addition, they slightly lower the R/Q of the resonance.

IMPEDANCE REDUCTION

Apart from the two RF systems, the vacuum flanges are the biggest resonant contributors to the longitudinal impedance of the SPS machine. These elements are, most likely, the culprits of the current instability problems of the SPS. For this reason, an impedance reduction campaign is under consideration for the Long Shutdown 2 (LS2) [4]. The objective is not only to reduce the impedance by damping the resonances, but also to reduce their R/Q in order to avoid the single bunch instability. To achieve this R/Q reduction, a modification of the interconnect geometry is needed. Two realistic options are currently under study.

Interconnect Redesign

Self-evidently, it is possible to redesign the flange and the attached bellows so that the overall longitudinal impedance is minimum. Two main modifications are needed to minimize the impedance of flanges belonging to group I. The gap between both flange sides is minimized, Fig. 3 (a), by

ISBN: 978-3-95450-168-7 doi:10.18429/JACoW-IPAC2015-MOPJE036

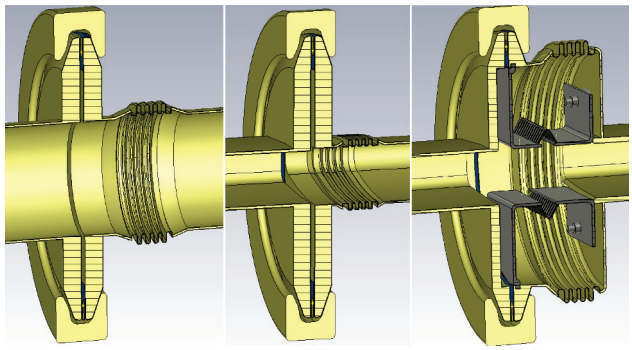

Figure 3: Possible modifications to the SPS vacuum flanges. (a) and (b) show the redesigned bellows for interconnects belonging to groups I and II, respectively. (c) Possible shield implementation for interconnects belonging to group II.

avoiding the current empty volume, Fig. 1 (a). Smooth transitions between the vacuum chamber and the bellows are implemented to avoid creating the current 'artificial' cavity. It has to be highlighted that, in some cases, the enamel isolation between both sides has to be kept. Therefore, the remaining gap of Fig. 3 (a) cannot be short-circuited. Table 2 compares the relevant impedance parameters for the 2.3 GHz resonance of a QD-QD flange. Both R/Q and Q_0 are greatly reduced, around factor 12 and 4 respectively.

Concerning flanges belonging to group II, to minimize the longitudinal impedance the current circular bellows (Fig. 1 (c)) would be replaced by 'elliptical' ones with smooth transitions to the vacuum chambers, Fig. 3 (b). In addition, as analogous to the previous case, the gap between both flange sides would be filled. Again, Table 2 compares the 1.4 GHz resonance parameters for the reference QF-QF flange. Not only the R/Q, but also the $\mathrm{Im}(Z)/n$ are reduced more than factor 10.

Table 2: Comparison between the different impedance reduction possibilities for the reference interconnects belonging to groups I and II.

		Non-enameled QD-QD	Non-enameled QF-QF
Current	R/Q	18 Ω	80 Ω
	Q_0	1400	270
	$\mathrm{Im}(Z)/n$	0.9 mΩ	3.5 mΩ
Redesign	R/Q	1.5 Ω	4.5 Ω
	Q_0	< 350	< 150
	$\mathrm{Im}(Z)/n$	0.25 mΩ	0.3 mΩ
Shielding	R/Q	–	8 – 12 Ω
	Q_0	–	< 100
	$\mathrm{Im}(Z)/n$	–	1.2 mΩ

Shielding

A cheaper alternative to producing elliptical bellows for the interconnects is to design an appropriate 'shield' as shown in Fig. 3 (c). In principle, this option is only viable for flanges belonging to group II. The proposed shielding could reduce the R/Q of the 1.4 GHz resonance by factor 7-10 and both the Q_0 and the $\mathrm{Im}(Z)/n$ to less than half. It has to be highlighted that, even though the shield heavily reduces the R/Q of the targeted resonance, it also creates a number of additional higher frequency resonances. This is the reason as to why the $\mathrm{Im}(Z)/n$ is much higher than the value obtained for the redesigned case. This issue has been studied recently and an improved shield implementation is currently under development.

CONCLUSIONS

The longitudinal coupling impedance of the SPS vacuum flanges has been studied in detail accounting for the 12 different types of interconnects. Simulation results have been crosschecked with measurements for the selected cases and very good agreement was found. The total contribution to the longitudinal impedance of the more than 600 elements has been calculated. Two possible ways of reducing the impedance have been presented. An impedance reduction campaign during LS2 is under consideration to overcome the current limitations.

ACKNOWLEDGMENT

The author wants to thank A. Grudiev, F. Caspers, E. Shaposhnikova, J. Perez and J. A. Ferreira for their help in various aspects related to this work including the damping resistor survey.

REFERENCES

[1] E. Shaposhnikova et al., "Identifiaction of High-Frequency Resonant Impedance in the CERN SPS", Proc. of IPAC2014, p. 1416-1418 (2014).

[2] G. Dôme, "Longitudinal Coupling Impedance of Cavities for a Relativistic Beam", Internal Note LABII/RF/Note/73-2, p. 1-14 (1973).

[3] E. Shaposhnikova, T. Bohl, T. Linnecar, "Results from the Impedance Reduction in the CERN SPS", 20^{th} ICFA Advanced Beam Dynamics Workshop, p. 62-64 (2002).

[4] "LHC Injectors Upgrade Technical Design Report" edited by J. Coupard et al., CERN-ACC-2014-0337 (2014).

[5] T. Argyropoulos, E. Shaposhnikova, J.E. Varela, "Other Means to Increase the SPS 25 ns Performance - Longitudinal Plane", LHC Performance Workshop, Chamonix (2014).

[6] ANSYS, "High Frequency Structural Simulator (HFSS) 15.0"

[7] "Computer Simulation Technology (CST) Stuido Suite 2014"

[8] O. Kononenko, A. Cappelletti and A. Grudiev, "Compensation of Transient Beam-Loading in CLIC Main Linac", Proc. of Linear Accelerator Conference, LINAC2010 (2010).

[9] G. Dôme, F. Caspers, "Precise Perturbation Measurements of Resonant Cavities and Higher Order Mode Identification", CERN SPS/85-46 (1984).